Incoherent pair tunneling in the pseudogap phase of cuprates

T. Micklitz,[1] A. Levchenko,[2] and M. R. Norman[3]

[1]*Dahlem Center for Complex Quantum Systems and Institut für Theoretische Physik, Freie Universität Berlin, 14195 Berlin, Germany*
[2]*Department of Physics and Astronomy, Michigan State University, East Lansing, Michigan 48824, USA*
[3]*Materials Science Division, Argonne National Laboratory, Argonne, Illinois 60439, USA*

Motivated by a recent experiment by Bergeal *et al.*, we reconsider incoherent pair tunneling in a cuprate junction formed from an optimally doped superconducting lead and an underdoped normal-metallic lead. We study the impact of the pseudogap on the pair tunneling by describing fermions in the underdoped lead with a model self-energy that has been developed to reproduce photoemission data. We find that the pseudogap causes an additional temperature-dependent suppression of the pair contribution to the tunneling current. We discuss consistency with available experimental data and propose future experimental directions.

PACS number(s): 74.50.+r, 74.72.Kf, 74.40.−n

I. INTRODUCTION

Upon lowering the temperature, the superconducting gap in underdoped cuprates evolves smoothly from an energy gap already present in the normal state.[1] Even after decades of debate, the nature of this "pseudogap" in the normal-metallic regime of the underdoped cuprates still remains a puzzle,[2] and new experiments are needed to shed light on its nature.

One such experiment was proposed by Janko *et al.*[3] The experimental setup consists of a junction formed by a superconducting and a normal-metallic lead in the pseudogap phase, separated by a tunneling barrier. If the pseudogap is due to the presence of preformed Cooper pairs, then the current-voltage (*I-V*) characteristics of such a junction should show characteristic signatures due to pair tunneling that differ from the standard result based on Gaussian fluctuations.[3]

The proposed experiment was recently done by Bergeal *et al.*,[4] and their data appear to be consistent with Gaussian fluctuations. However, even if preformed pairs is not a correct description, the pseudogap, regardless of its origin, still affects the fermions in the normal-metallic lead, and thereby the Gaussian result should not hold. A similar observation has recently been made in the context of the Nernst effect in the pseudogap phase of underdoped cuprates.[5] Current vertices calculated within a model that reproduces photoemission data in the pseudogap phase[6,7] show an additional temperature dependence, which suppresses the Nernst signal relative to the Gaussian result, consistent with experimental data.

In the present paper, we study whether a similar effect of the pseudogap changes the *I-V* characteristics in the above-mentioned tunnel junction. We compare with experimental findings by Bergeal *et al.* and discuss possible further directions to improve the understanding of the incoherent pair tunneling in the pseudogap phase of cuprates. Throughout the paper, we set $\hbar = 1$ and $k_B = 1$.

II. FLUCTUATING PAIR TUNNELING

A direct experimental test of pairing fluctuations above T_c is the second-order Josephson effect,[3,8–11] which has been observed in conventional superconductors[12] and, more recently, in cuprates.[4] The effect is exhibited in a junction involving two leads, in the cuprate case, with one underdoped

(UD) and the other optimally doped (OD), with critical temperatures such that $T_c^{\rm UD} < T < T_c^{\rm OD}$. The rigid pair field of the optimally doped superconductor then plays the role of the external field in a typical (linear response) susceptibility measurement.

The net effect is that the fluctuating pairs produce an additional contribution $I_{\rm pair}$ to the current-voltage characteristics of the junction that is directly proportional to the imaginary part of the pair susceptibility χ of the pseudogap lead,

$$I_{\rm pair}(V,H) \propto e\,\mathcal{C}^2 \chi''[q(H),\omega(V)]. \tag{1}$$

Here the frequency $\omega(V) = 2\,{\rm eV}$ is linear in the bias voltage V, and momentum $q(H)$ is linear in the in-plane magnetic field H. The magnitude of the pair contribution to the tunneling current is controlled by the vertex $\mathcal{C}$, which describes the pair transfer between the leads and depends on the specifics of the junction. A measurement of the excess current $I_{\rm pair}$ as a function of V and H allows one to trace the frequency and momentum dependencies of the fluctuating pair susceptibility.

A. Microscopic theory

In a microscopic calculation, the lowest-order pair contribution to the tunneling current arises in fourth-order perturbation theory,[9,14] diagrammatically depicted in Fig. 1. Assuming a particle-particle t matrix for the pseudogap lead with pairing instability in the d-wave channel, and keeping only the relevant d-wave part of the tunneling matrix element, the incoherent pair contribution to the tunneling current is of the form (see Fig. 1 for details)

$$I_{\rm pair}(V,H) = 4eSa^2\,\mathcal{C}^2 \chi''[q(H),\omega(V)], \tag{2}$$

where $\chi''(\mathbf{q},\omega) = {\rm Im}\mathcal{L}_{\mathbf{q}}^R(\omega)$, with $\mathcal{L}^R$ the retarded component of the fluctuating pair propagator, V and H the applied voltage and in-plane magnetic field, and S and a^2 the junction area and the lattice spacing, respectively. The vertex

$$\mathcal{C} = \frac{\gamma T}{N^2} \sum_{\epsilon_n} \sum_{\mathbf{p},\mathbf{k}} F_{\mathbf{p}}^{\rm sc}(i\epsilon_n,\Delta_A) G_{\mathbf{k}}(i\epsilon_n) G_{-\mathbf{k}}(-i\epsilon_n)$$
$$\times \cos(2\varphi_{\mathbf{p}})\cos^2(2\varphi_{\mathbf{k}}) \tag{3}$$

describes the tunneling of an incoherent pair[3] and sets the magnitude of the pair current. We assume that the c axis is
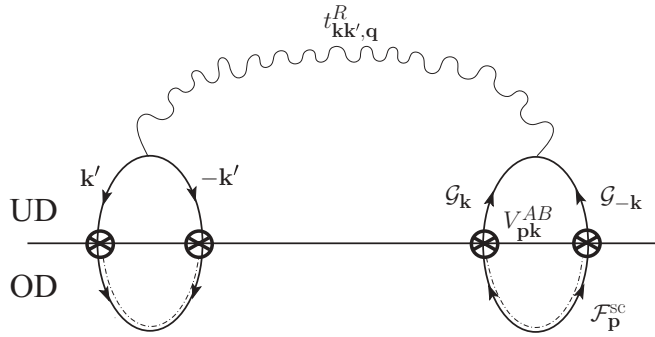
FIG. 1. Incoherent pair tunneling contribution, $I_{\mathrm{pair}} = 2e\,\mathrm{tr}(F^A V^{AB} G^B G^B t^B G^B G^B V^{BA} F^A)$, to the tunneling current. Here the trace includes summations over momenta and frequencies; double and single lines correspond, respectively, to Gor'kov functions $F_{\mathbf{p}}^A(i\epsilon_n)$ of the optimally doped (OD) lead A and single-particle Greens functions $G_{\mathbf{k}}^B(i\epsilon_n)$ of the underdoped (UD) pseudogap lead B; circles represent one-electron tunneling matrix elements $V_{\mathbf{pk}}^{AB}$,[13] and the wavy line denotes the particle-particle t matrix for the pseudogap lead B (here for $\mathbf{q} = 0$). To arrive at Eq. (2) in the text, we assumed a pairing instability in the d-wave channel, $t_{\mathbf{k,k',q}}^R(\omega) = \mathcal{L}_{\mathbf{q}}^R(\omega)\cos(2\varphi_{\mathbf{k}})\cos(2\varphi_{\mathbf{k'}})$, and kept only the relevant d-wave part $\propto V_1$ in the harmonic expansion of the tunneling matrix elements, $\langle|V_{\mathbf{pk}}^{AB}|^2\rangle = |V_0|^2 + |V_1|^2\cos(2\varphi_{\mathbf{p}})\cos(2\varphi_{\mathbf{k}})$; see Refs. 3 and 13.

perpendicular to the junction, and all momenta and coordinates contain only two-dimensional in-plane components. Here

$$F_{\mathbf{p}}^{\mathrm{sc}}(i\epsilon_n,\Delta) = \frac{\Delta_{\mathbf{p}}}{\epsilon_n^2 + \xi_{\mathbf{p}}^2 + \Delta_{\mathbf{p}}^2} \qquad (4)$$

denotes the anomalous Gor'kov function of the superconducting lead A, with ϵ_n (fermionic) Matsubara frequencies, $\Delta_{\mathbf{p}} = \Delta\cos(2\varphi_{\mathbf{p}})$ with $\varphi_{\mathbf{p}} = \arctan(p_y/p_x)$, and $G_{\mathbf{k}}(i\epsilon_n)$ is the single-particle propagator of the pseudogap lead B (specified below). Finally, $\gamma = n_i|V_1|^2/N^2$, with N the number of sites in a layer and n_i the number of impurity scattering sites per unit area of the insulating junction. $|V_1|$ is defined in Fig. 1.[3]

The precise form of the pair susceptibility χ varies depending on the particular scenario adopted to describe the pseudogap phase. In this paper, we will adopt the standard Gaussian form for the pair propagator,

$$\mathcal{L}_{\mathbf{q}}^R(\omega) = -\frac{1}{N_0}\frac{1}{\epsilon - i\alpha\omega + \eta q^2}. \qquad (5)$$

Here, $\epsilon = (T - T_c)/T_c$, N_0 is the density of states, $\alpha = \pi/8T$, and $\eta = \pi D/8T$, where D is the diffusion constant. Alternate forms, where α is complex (in a preformed-pairs scenario due to a BCS-BEC crossover between diffusive and propagating pairs)[3,15,16] seems to be ruled out by Bergeal et al.[4]

However, even if the pseudogap is not due to preformed pairs and a Gaussian approach [Eq. (5)] is relevant, the pseudogap will still affect the tunneling current through the vertex $\mathcal{C}$. A similar observation has recently been made in the context of the Nernst effect in the pseudogap phase of underdoped cuprates.[5] Calculation of the current vertices within a model[6,7] which reproduces photoemission data in the pseudogap phase leads to an additional T-dependent suppression of the Nernst effect relative to that predicted

by the Gaussian model, consistent with experimental data. We will now determine if a similar modification occurs for the tunneling current, independent of whether or not the pseudogap is due to pairing. Before doing so, we recall that within the GG_0 approximation employed by Janko et al.,[3] the vertex is

$$\mathcal{C} \simeq \frac{\pi^2}{4}n_i|V_1|^2 N_A(0)N_B(0), \qquad (6)$$

with $N_A(0)$ and $N_B(0)$ the single-particle density of states per spin per site for superconducting lead A and pseudogap lead B, respectively.

B. Pseudogap vertex

We next investigate implications of the the pseudogap for the pair tunneling. Following Refs. 5 and 17, we calculate the vertex (3) using the Greens function,

$$G_{\mathbf{k}}(i\epsilon_n,\Delta_B) = \frac{i\bar{\epsilon}_{0,n} + \xi_{\mathbf{k}}}{(i\bar{\epsilon}_{1,n} - \xi_{\mathbf{k}})(i\bar{\epsilon}_{0,n} + \xi_{\mathbf{k}}) - \Delta_{B,\mathbf{k}}^2}, \qquad (7)$$

which is based on a phenomenological self-energy describing photoemission data in the pseudogap phase.[6,7] Here, $\Delta_{\mathbf{k}} = \Delta\cos(2\varphi_{\mathbf{k}})$ is the momentum-dependent pseudogap, $\xi_{\mathbf{k}}$ are the single-particle energies measured from the Fermi level μ, and $(i = 0,1)$ $\bar{\epsilon}_{i,n} = \epsilon_n + \Gamma_i\,\mathrm{sign}(\epsilon_n)$, with Γ_0 the inverse pair lifetime proportional to $T - T_c$ (i.e., ϵ/α), and Γ_1 the single-particle scattering rate. For $\Gamma = \Gamma_1 = \Gamma_0$, Eq. (7) reduces to the single-lifetime model,

$$G_{\mathbf{k}}(i\epsilon_n,\Delta_B) = -\frac{i\bar{\epsilon}_n + \xi_{\mathbf{k}}}{\bar{\epsilon}_n^2 + \xi_{\mathbf{k}}^2 + \Delta_{B,\mathbf{k}}^2}. \qquad (8)$$

Equation (8) gives a good description of the T dependence of the Fermi arc if $\Gamma \propto T$.[7]

To compute the vertex (3), we first derive that the momentum sum for the two-lifetime model is

$$N^{-1}\sum_{\mathbf{k}} G_{\mathbf{k}}(i\epsilon_n)G_{-\mathbf{k}}(-i\epsilon_n)\cos^2(2\varphi_{\mathbf{k}})$$

$$= \frac{N_B(0)}{\Delta_B}\frac{X_n}{2}\left\{\frac{1}{X_n^2}[E(X_n) - K(X_n)]\right.$$

$$\left. + \left[1 + Z_{0,n}^2\right]K(X_n) - Y_n^2 Z_{1,n} Z_{0,n}^3 \Pi(Y_n,X_n)\right\}$$

$$\equiv \frac{N_B(0)}{\Delta_B}\mathcal{M}^{\mathrm{pg}}(T,\Gamma_0,\Gamma_1,\Delta_B), \qquad (9)$$

where we introduced

$$\frac{1}{X_n^2} = 1 + \frac{(\Gamma_0 - \Gamma_1)^2}{4\Delta_B^2} + \frac{\bar{\epsilon}_{1,n}\bar{\epsilon}_{0,n}}{\Delta_B^2}, \qquad (10)$$

$$\frac{1}{Y_n^2} = 1 + \frac{\bar{\epsilon}_{1,n}\bar{\epsilon}_{0,n}}{\Delta_B^2}, \qquad (11)$$

$$Z_{i,n} = \frac{\bar{\epsilon}_{i,n}}{\Delta_B}, \qquad (12)$$

and $K(z)$, $E(z)$, and $\Pi(w,z)$ are the complete elliptic integrals of the first, second, and third kind, respectively.

The momentum sum over the Gor'kov Greens function, on the other hand, is

$$N^{-1} \sum_{\mathbf{p}} F_{\mathbf{p}}^{\text{sc}}(i\epsilon_n, \Delta_A) \cos(2\varphi_{\mathbf{p}})$$

$$= N_A(0)k_n \left\{ E(k_n) + \frac{\epsilon_n^2}{\Delta_A^2} [E(k_n) - K(k_n)] \right\}$$

$$\equiv N_A(0)\mathcal{M}^{\text{sc}}(T, \Delta_A), \tag{13}$$

where $k_n^2 = 1/(1 + \epsilon_n^2/\Delta_A^2)$.

The vertex is then obtained by completing the Matsubara sum,

$$\mathcal{C} = \frac{3\pi^2}{32} n_i |V_1|^2 N_A(0) N_B(0) \mathcal{A}(T, \Gamma_0, \Gamma_1, \Delta_A, \Delta_B). \tag{14}$$

Here we have included the numerical prefactor for later convenience, and the temperature-dependent, dimensionless function

$$\mathcal{A}(T, \Gamma_0, \Gamma_1, \Delta_A, \Delta_B)$$

$$= \frac{32}{3\pi^2} \frac{T}{\Delta_B} \sum_n \mathcal{M}^{\text{sc}}(T, \Delta_A) \mathcal{M}^{\text{pg}}(T, \Gamma_0, \Gamma_1, \Delta_B). \tag{15}$$

It may then be verified that approximating in $\mathcal{A}$ the elliptic functions by their value at zero argument describes well the temperature dependence of Eq. (15) (see below). Using that the elliptic functions at zero argument take the value $\pi/2$, we may thus approximate $\mathcal{A}(T, \Gamma_0, \Gamma_1, \Delta_A, \Delta_B) \simeq \mathcal{A}_1(T/\Delta_B, \Gamma_0/\Delta_B, \Gamma_1/\Delta_B, \Delta_A/\Delta_B)$, where the temperature-dependent function, normalized as $\mathcal{A}_1(0,0,0,1) = 1$, $(z_n = \epsilon_n/\Delta_B)$, is

$$\mathcal{A}_1(x_0, x_1, x_2, x_3) = \frac{4x_3 x_0}{3} \sum_n \frac{(z_n + x_1)[2z_n + x_2 + x_1] + 1}{\left\{ [z_n^2 + x_3][(z_n + x_2)(z_n + x_1) + \frac{(x_1 - x_2)^2}{4} + 1)] \right\}^{1/2} [(z_n + x_2)(z_n + x_1) + 1]}. \tag{16}$$

In the single-lifetime model, we may introduce the corresponding functions $\mathcal{B}(T, \Gamma, \Delta_A, \Delta_B) \equiv \mathcal{A}(T, \Gamma, \Gamma, \Delta_A, \Delta_B)$ and, analogously, $\mathcal{B}_1(T/\Delta_B, \Gamma/\Delta_B, \Delta_A/\Delta_B)$ for Eq. (16) in the same limit. As can be verified (see below), taking the "zero-T" limit in order to convert the sum over Matsubara frequencies into an integral gives a good description of the vertex in the single-lifetime model. We may thus further approximate $\mathcal{B}(T, \Gamma, \Delta_A, \Delta_B) \simeq \mathcal{B}_0(\Gamma/\Delta_B, \Delta_A/\Delta_B)$, where

$$\mathcal{B}_0(x_1, x_3) = \frac{4x_3}{3\pi} \int_0^\infty dz \frac{2(z + x_1)^2 + 1}{\sqrt{z^2 + x_3}[(z + x_1)^2 + 1]^{3/2}}. \tag{17}$$

Comparing then to Eq. (6) in the previous section, we find that taking into account the pseudogap within the two- and single-lifetime models (7) and (8) results in a renormalization of the pair contribution to the tunneling current by the T-dependent functions, $\mathcal{A}^2(T, \Gamma_0, \Gamma_1, \Delta_A, \Delta_B)$ and $\mathcal{B}^2(T, \Gamma, \Delta_A, \Delta_B)$ (their approximations $\mathcal{A}_1^2$ and $\mathcal{B}_0^2$, respectively).

So far we have neglected any external magnetic fields. The variation of an in-plane field allows one to trace the momentum dependence of the fluctuating pair propagator; see Eq. (2). If the relevant field scale on which the pair contribution gets suppressed is small enough so as to not affect the single-particle contribution, then the magnetic field allows one to separate these two contributions to the tunneling current. We will address this matter further in the next section.

C. Comparison to experiment

The recent tunneling experiment by Bergeal *et al.*[4] using a YBa$_2$Cu$_3$O$_{6+x}$/NdBa$_2$Cu$_3$O$_{6+x}$ (YBCO/NdBCO) junction with optimally doped (OD) NdBCO and underdoped (UD) YBCO was designed to test Eq. (5) and alternate forms suggested by Janko *et al.*[3] The corresponding critical temperatures, $T_c^{\text{OD}} = 90$ K and $T_c^{\text{UD}} \simeq 61$ K (the pseudogap temperature for the UD sample is $T^* \simeq 250$ K), allow for a comparison to predictions in a range of temperatures extending

over a considerable fraction of T_c. Provided the vertex $\mathcal{C}$ changes only weakly with temperature, the data reported by Bergeal *et al.* are consistent with a standard model of Gaussian fluctuations with a susceptibility given by Eq. (5),

$$\chi''(q, \omega) \propto \frac{\alpha\omega}{(\epsilon + \eta q^2)^2 + (\alpha\omega)^2}. \tag{18}$$

The extracted pair contribution to the tunneling current is in good agreement with a Lorentzian with a width that was 1.6 times $\Gamma_{\text{GL}} = 8(T - T_c)/\pi$ at $T - T_c = 6$ K and 1.3 times at $T - T_c = 9$ K. This is in good accord with angle-resolved photoelectron spectroscopy (ARPES), where Γ_0 was found to be approximately twice Γ_{GL}.[6]

The vertex renormalization within the single-lifetime model, $\mathcal{B}^2(T, \Gamma, \Delta_A, \Delta_B)$, is depicted in Fig. 2 for a T-independent maximal value of the energy gap in the superconducting and pseudogap phase $\Delta_A \simeq \Delta_B = \Delta$, with Γ scaling as T. The scaling factor used to describe the photoemission data is $\Gamma/\Delta = \sqrt{3}T/T^*$, implying that the T dependence of $\mathcal{B}^2(T, \Gamma, \Delta_A, \Delta_B)$ is controlled by the pseudogap temperature T^* (at which the spectral gap "fills up" in the antinodal region of the Brillouin zone). For the UD sample, $T^* \simeq 250$ K, and the temperature range in which pair tunneling is detected by Bergeal *et al.* ($\sim$15 K) is too narrow to observe any noticeable deviations from predictions of the simple Gaussian formula (18). To test the predicted rapid suppression at higher temperatures coming from $\mathcal{B}^2(T, \Gamma, \Delta_A, \Delta_B)$ will require using a magnetic field to cleanly separate the pair tunneling current from the much larger normal tunneling current.

Within the two-lifetime model, the vertex renormalization depends on the ratios Γ_0/Δ_B and Γ_1/Δ_B. Since Γ_0 has a rapid T dependence near T_c, one might suspect a stronger effect as compared to the single-lifetime model. From (15), one finds, however, that for any reasonable value of Γ_1/Δ comparable to that found from photoemission, the dependence of $\mathcal{A}^2(T, \Gamma_0, \Gamma_1, \Delta_A, \Delta_B)$ on temperature is qualitatively
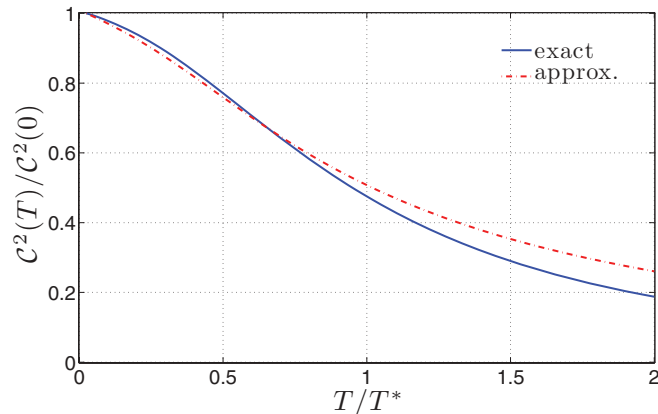
FIG. 2. (Color online) T dependence of the vertex $\mathcal{C}^2$ within the single-lifetime model for the pseudogap lead, where $\mathcal{C} \propto \mathcal{B}(T, \Gamma, \Delta_A, \Delta_B)$. Here T^* is the pseudogap temperature, $\Delta_A \simeq \Delta_B = \Delta$, and $\Gamma/\Delta = \sqrt{3}T/T^*$, so that the Fermi arcs connect at $T = T^*$. The solid line shows the exact result with $\mathcal{B}$ given in (15) and $\Gamma_0 = \Gamma_1 = \Gamma$, and the dash-dotted line shows the approximation $\mathcal{B}_0$ given in (17).
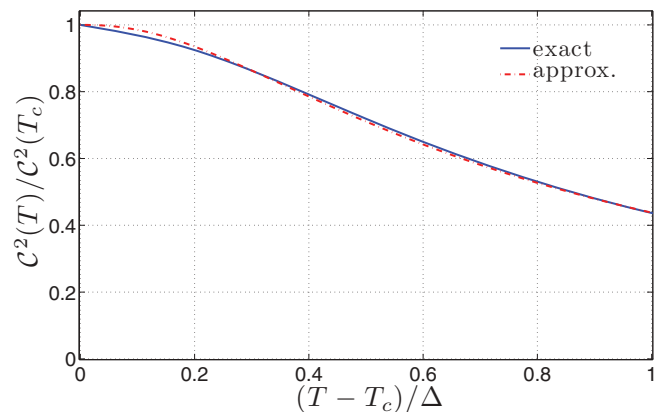

FIG. 3. (Color online) T dependence of the vertex $\mathcal{C}^2$ within the two-lifetime model for the pseudogap lead, where $\mathcal{C} \propto \mathcal{A}(T, \Gamma_0, \Gamma_1, \Delta_A, \Delta_B)$. Here, $\Delta_A \simeq \Delta_B = \Delta$ and parameters similar to Ref. 6, $\Gamma_1 = 200$ meV, $\Delta = 50$ meV, and $\Gamma_0 = (16/\pi)(T - T_c)$, twice Γ_{GL}, where $T_c = 80$ K. The solid line shows the exact result $\mathcal{A}$ given in (15) and the dash-dotted line shows the approximation $\mathcal{A}_1$ given in (16).

similar to that in the single-lifetime model; see Fig. 3. It becomes more pronounced only for small values of $\Gamma_1/\Delta \ll 1$. We note that a zero-T approximation similar to (17) is not applicable for the two-lifetime model.

Finally, some remarks are made about the magnetic field dependence. The length scale which sets the Fraunhofer pattern (i.e., the field dependence) of the Josephson current is $Z = X_A + X_B + d$, where $X = \lambda \tanh(W/2\lambda)$, with $\lambda_{A,B}$ and $W_{A/B}$ the a/b penetration depth and thickness of films A and B, respectively, and d the thickness of the barrier.[18] In the two limits of wide and thin films, $X(\lambda, W) \simeq \lambda$ and $X(\lambda, W) \simeq W/2$, respectively. Referring then to the experimental configuration of Bergeal *et al.*, $W_A = 200$ nm, $W_B = 100$ nm, $d = 30$ nm, and the junction length $L = 5000$ nm. For the optimally doped superconducting film, (A) $\lambda_A = 100$ nm, and for the underdoped film, (B) $\lambda_B = 200$ nm, if it were superconducting. However, the latter is above T_c^{UD} and has no long-range order, i.e., lead B is in the thin-film limit $X_B \simeq W_B/2$. Therefore, $X_A = \lambda_A \tanh(W_A/2\lambda_A) \simeq 76$ nm and $Z = X_A + W_B/2 + d \simeq 156$ nm. The corresponding field scale H is then estimated from $HLZ = \phi_0$, where ϕ_0 is the flux quantum, yielding $H \simeq 25$ Gauss. Since the normal contribution to the current should not change much at a field of 25 Gauss, while the pair contribution is strongly suppressed at this field, this allows one to distinguish the two contributions. This could be exploited in future experiments.

In this context, notice that in contrast to YBCO, in the case of $\mathrm{Bi_2Sr_2CaCu_2O_{8+x}}$ (suggested by Janko *et al.*),[3] one has a stack of Josephson junctions. The effect due to the stack would be to create a new length scale Z' equal to the bilayer-bilayer separation,[19] which is of the order ~ 1.5 nm. The resulting small length scale corresponds to a field scale H for the stack about two orders of magnitude

larger than Z, meaning that the presence of a stack would not affect the I-V characteristics of the A-B junction on the field scale discussed above, and thus this complication can be ignored.

III. SUMMARY

Implications of the pseudogap on transport[17] and the Nernst effect[5] have been previously studied within a phenomenological model used to describe photoemission data. Here we study the implications of the pseudogap on the pair tunneling, as recently measured by Bergeal *et al.*[4] We find that accounting for the pseudogap within a single-lifetime model leads to a suppression of the pair contribution to the tunneling current relative to Gaussian theory as the temperature is increased. Within the rather small temperature range tested in the experiment, however, this effect would not be noticeable. To determine this would require differentiating the pair current from the much larger normal current, which would require the application of a small in-plane magnetic field. We contrast this with the Nernst effect, where the normal background is significantly smaller. Therefore, we suggest that such field-dependent measurements be done in the future; this would not only help identify effects due to the vertex, but also would test the validity of Eq. (5) in the context of specific theories for the pseudogap phase.[20]

[1]T. Timusk and B. Statt, Rep. Prog. Phys. **62**, 61 (1999).
[2]M. R. Norman, D. Pines, and C. Kallin, Adv. Phys. **54**, 715 (2005).

[3]B. Janko, I. Kosztin, K. Levin, M. R. Norman, and D. J. Scalapino, Phys. Rev. Lett. **82**, 4304 (1999).

[4]N. Bergeal, J. Lesueur, M. Aprili, G. Faini, J. P. Contour, and B. Leridon, Nature Phys. **4**, 608 (2008).

[5]A. Levchenko, M. R. Norman, and A. A. Varlamov, Phys. Rev. B **83**, 020506 (2011).

[6]M. R. Norman, M. Randeria, H. Ding, and J. C. Campuzano, Phys. Rev. B **57**, R11093 (1998).

[7]M. R. Norman, A. Kanigel, M. Randeria, U. Chatterjee, and J. C. Campuzano, Phys. Rev. B **76**, 174501 (2007).

[8]D. J. Scalapino, Phys. Rev. Lett. **24**, 1052 (1970).

[9]S. R. Shenoy and P. A. Lee, Phys. Rev. B **10**, 2744 (1974).

[10]X. Dai, T. Xiang, T.-K. Ng, and Z.-B. Su, Phys. Rev. Lett. **85**, 3009 (2000).

[11]A. Levchenko, Phys. Rev. B **78**, 104507 (2008).

[12]J. T. Anderson and A. M. Goldman, Phys. Rev. Lett. **25**, 743 (1970).

[13]In the above experiment, it is assumed that tunneling takes place via direct or resonant processes through localized states in the barrier, and $\langle |V^{AB}|^2 \rangle$ is the impurity-averaged single-electron transfer through the diffusive tunneling barrier.

[14]H. Takayama, Progr. Theor. Phys. **46**, 1 (1971).

[15]A. Perali, P. Pieri, G. C. Strinati, and C. Castellani, Phys. Rev. B **66**, 024510 (2002).

[16]J. Maly, B. Janko, and K. Levin, Physica C **321**, 113 (1999).

[17]A. Levchenko, T. Micklitz, M. R. Norman, and I. Paul, Phys. Rev. B **82**, 060502 (2010).

[18]M. Weihnacht, Phys. Stat. Sol. **32**, K169 (1969).

[19]R. Kleiner and P. Müller, Phys. Rev. B **49**, 1327 (1994).

[20]J.-H. She, B. J. Overbosch, Y.-W. Sun, Y. Liu, K. E. Schalm, J. A. Mydosh, and J. Zaanen, Phys. Rev. B **84**, 144527 (2011).